Wireless Aquatic Navigator for Detection and Analysis (WANDA)

Cormac Fay[a], King-Tong Lau[a], Stephen Beirne[a], Ciarán Ó Conaire[a], Kevin Mc Guinness[a], Brian Corcoran[a], Noel E. O'Connor[a] and Dermot Diamond[a*]
[a]CLARITY: Centre for Sensor Web Technologies, Dublin City University, Glasnevin, Dublin 9, Ireland.

Scott McGovern[b], Greg Coleman[b], Rod Shepherd[b], Gursel Alici[b], Geoff Spinks[b] and Gordon Wallace[b]
[b]Intelligent Polymer Research Institute, ARC Centre of Excellence for Electromaterials Science, University of Wollongong, NSW, Australia.

Abstract.

The cost of monitoring and detecting pollutants in natural waters is of major concern. Current and forthcoming bodies of legislation will continue to drive demand for spatial and selective monitoring of our environment, as the focus increasingly moves towards effective enforcement of legislation through detection of harmful events, and unambiguous identification of perpetrators. However, these monitoring demands are not being met due to the infrastructure and maintenance costs of conventional sensing models. Advanced autonomous platforms capable of performing complex analytical measurements at remote locations still require individual power, wireless communication, processor and electronic transducer units, along with regular maintenance visits. Hence the cost base for these systems is prohibitively high, and the spatial density and frequency of measurements are insufficient to meet requirements. In this paper we present a more cost effective approach for water quality monitoring using a low cost mobile sensing/communications platform together with very low cost stand-alone 'satellite' indicator stations that have an integrated colorimetric sensing material. The mobile platform is equipped with a wireless video camera that is used to interrogate each station to harvest information about the water quality. In simulation experiments, the first cycle of measurements is carried out to identify a 'normal' condition followed by a second cycle during which the platform successfully detected and communicated the presence of a chemical contaminant that had been localised at one of the satellite stations.

Keywords: Water Monitoring, Polymer Actuator, Wireless Sensing, Biomimetics, pH Detection, Optical Sensing, Digital Imaging, Colorimetric Reagent

* Corresponding Author: dermot.diamond@dcu.ie

1. INTRODUCTION

It has been long recognised that the interaction between industrialised societies and the environment can be negative, in that concentrations of people in urbanised areas, with co-located industries will have a negative impact on the overall quality of the environment. An important aspect of this interaction is the release of pollutants into local water bodies, such as rivers and lakes, which can adversely affect the health of people and cause devastating fish kills [1-6]. Consequently, environmental protection is a priority in modern society, and an extensive, and growing, body of legislation exists that specifies the limits of key chemical and biological pollutants in various types of water (potable, drinking, ground etc.) [7-9].

Arising from the enforcement of this body of legislation is a growing need to police these pollutant limits, through analytical measurements that are used to determine the water quality [10]. However, these measurements are almost always achieved by taking samples from a relatively small number of designated locations, and analysing the composition at a centralised laboratory facility equipped with sophisticated state-of-the-art equipment. There are good reasons for employing this strategy, principally because of the high precision and accuracy of the measurements, which are vital for obtaining legally binding decisions against polluters. However, because of the expense involved to manage the analytical facilities and monitoring programmes, this model is inherently not scalable, and measurements are very restricted in terms of the number of locations and sampling frequency [11, 12].

In recent years, we have developed autonomous analyser platforms that can perform complex analytical measurements at remote locations, and make the resulting data globally available via websites. However, the cost base for these devices is still relatively high as it includes pumps, valves, microfluidics, optical detection, reagents, standards, electronics, power, and wireless communications, all housed within a robust enclosure [13-15]. In this paper, we present a radically different approach to remote water quality monitoring based on a low cost, biomimetic robotic fish, known as WANDA (Wireless Aquatic Navigator for Detection and Analysis). The WANDA platform is capable of movement via a polymer actuator based tailfin [16], and can report what it 'sees' via an integrated low-power wireless video camera. The biomimetic fish can be used in conjunction with very low-cost, dispersed, colorimetric 'satellite' sensors integrated into an easily recognised 3D form that enable very effective shape-identification algorithms [17] to be employed to distinguish the sensor from its surroundings. Once the sensor has been located, the camera is used to interrogate its condition and make the resulting data available via a wireless link. In this manner, a single, low power robotic platform can harvest analytical information about the local chemical and/or biological environment at multiple locations using very low cost sensors.

In this paper, we demonstrate the principle of this approach using dispersed colorimetric sensors to probe changes in the local pH at several locations. Specifically, a water container of sufficient size (to allow for manoeuvrability) is setup within a laboratory setting. Several colorimetric sensors are then dispersed within the water container whereby an initial sensing patrol by WANDA allows for reference measurements of the sensors in uncontaminated conditions. A subsequent sensing patrol takes place whereby the water surrounding one station is acidified, resulting in a colorimetric change that is sensed by the camera. The results of the two patrols are compared showing that a change in pH has occurred in the water surrounding the station.

2. ROBOTIC FISH PLATFORM

The mobile wireless sensor platform used combines many disciplines into one practical device including materials science, wireless communications, vision systems, chemistry, systems control, biomimetics and robotics. However, in this paper, we will focus on three of these;

- the biomimetic novel propulsion method;
- the ability to navigate and sense chemical events and;
- system construction and control.

2.1 Propulsion Method

Conducting polymer actuators (or artificial muscles) based on polypyrrole (PPy) [18] have been utilised within the propulsive element of the tail fin of WANDA. With the application of an oscillating voltage (e.g. a low voltage square wave, +/- 1V 1Hz), a bi-directional bending movement is derived from the actuators as one side becomes oxidised, and the other side is reduced. This oxidation/reduction process is accompanied by swelling/contraction of the respective polymer layers, due to movement of anions and water of hydration associated with the maintenance of overall charge neutrality, see Figure 1a. In such a system, the direction of bending is controlled by the polarity of the applied voltage. If a rigid tail fin is attached to a pair of actuators (Figure 1b) the force generated can enable a transfer of energy from the bending motion of the actuator to the water.

2.2 Navigation and Sensing

The WANDA platform is equipped with a wireless video camera for two main purposes. The first is for navigation as, through the video images, one can estimate the location of the device while building a map of the environment. This technique, known as Simultaneous Localization And Mapping (SLAM), has received continuous attention for the last two decades [19, 20].

The second purpose of the onboard camera is to harvest information about the chemistry of the water body it is moving through. In this study, we achieve this through the use of a number of sensing stations fitted with a chemo-responsive dye which responds colorimetrically to changes in the chemistry of the local environment. By using the onboard camera, a mobile device can easily detect differences in colour and in turn this can be related to the levels of certain chemicals in that region of the water body. Previous works [21-25] have shown that it is possible to monitor changes of pH in a laboratory using a colour camera, and we have therefore selected this measurement as the proof of principle test for the platform.

2.3 System construction and control

A primary goal for the research was to control the movement of WANDA using a biomimetic polymer actuator. Figure 2 shows the assembly of the WANDA fish platform presented in schematic (Figure 2a) and photographic (Figure 2b) formats for clarity. The main components, i.e. wireless camera and control circuitry, are housed within a waterproof container (a truncated 50 ml syringe). Connected to the casing's bung are the PPy actuators to which the tailfin cut from a thin plastic sheet is attached. The range of the WANDA device is dictated by the wireless camera allowing for a

transmission length of 100 m [26] The control circuitry is powered from the wireless camera's battery allowing for a continuous operation (PPy bidirectional actuation of 1 Hz with wireless video transmission) of WANDA for a period of ca. 3.5 hours in its current configuration.

By coupling the propulsion method with machine vision techniques, autonomous control is achievable. Further, by interpreting the scene with data captured by the onboard camera using a combination of image processing algorithms, WANDA can avoid obstacles, track towards objects of interest and/or perform chemical analysis. To achieve this, commands are sent from the base station to the tailfin control circuitry on board WANDA (Figure 3) and in turn alter the tailfin's state, resulting in motion.

In this study, WANDA moves through a fixed patrol route in a water container under remote control from the base station. When a chemical indicator station comes within the camera's field of view, colorimetric analysis is performed on the pixels representing the chemically responsive dye. This returns a quantitative estimation of the pH of the immediate environment surrounding the chemical indicator station.

3. EXPERIMENTAL

3.1 Materials and Equipment

A standard colour reference chart (X-Rite Colour Checker Passport) is used as reference for colorimetric analysis. The wireless camera (ZTV ZT830T) transmits a video stream from WANDA to the receiver (AEE AR101 placed ca. 4 m from the water container), which forwards it to the video capture card (Avermedia C038). The main processor (Dell Latitude D630) interrogates the signal and sends a direction command via radio (EZ Radio ER900TRS 250 m possible range [27]) to the microcontroller (PIC16F683) on WANDA which in turn controls the tailfin (polypyrrole) movement.

The water container (Intex 59416NP) used for experimentation, was cylindrically shaped with a diameter of 114 cm, a height of 25 cm and filled 8 cm with water allowing sufficient room for WANDA to manoeuvre. 1 Molar HCl solution was made from 37 % HCl (Scharlau AC0741) and ultra pure water (Millipore Milli-Q), and this was used to change the local pH near one of the pH sensing stations.

Three identical pH sensing stations were constructed as shown in Figure 4. The stations consist of a standard 20 ml vial affixed (Loctite 3430) to a heavy metallic base with a strip of Universal Indicator (Johnson Universal pH Indicator) attached around the centre of the vial. The strip was modified with ethyl cellulose (Sigma-Aldrich 28244) to reduce leaching effects. This was achieved by dissolving 100 mg of ethyl cellulose in 10 ml of solvent (ethanol). After manually coating the strip, a thin layer of porous ethyl cellulose resulted allowing efficient exchange of H+ ions but inhibits loss of the much larger dye molecules.

Software components used as part of overall system integration include:

- Java Runtime Edition [28] – Standard Java Programming Package
- Javax.comm [29] – Serial Port Communications

- Direct Show Java (DSJ) [30] – Video Capture
- Java Advanced Imaging [31] – Video Processing & Analysis

3.2 Image Processing

The video stream is captured from the capture card at a standard size of 640 x 480 pixels, 15 frames per second (fps), 24-bit colour depth (8x8x8) in raw RGB format as artefacts arising from compression algorithms (such as the MPEG family) may distort the estimated values. Figure 5a shows a captured image of a submerged sensor station. For colorimetric analysis, it is necessary to extract the image region representing the pH sensing strip (see Figure 4). To achieve this (Figure 5c) a number of image processing steps were combined to segment the region of interest (i.e. to identify all pixels that represent the pH chemo-responsive material of the sensor station). Firstly, a region of interest is selected containing the indicator material and background. After that, to aid in the segmentation process, noise reduction techniques were applied; a median filter [32] followed by a standard 3x3 grey level morphological dilation [33]. Subsequently, a transformation from the RGB colour space to the HSI colour space [34] is performed to assist colorimetric analysis i.e. to investigate if a more robust model to variable lighting intensities can be used, see Section 4.1. Since the pH material will only change colour between green and red when acid is introduced (Figure 6), a band pass filter was applied to the Hue channel (from 0 rad to 2.09 rad, see Figure 7 for quantitative values in relation to colours[35]). Next, a standard region labelling algorithm was applied to the Hue channel. This gave a grey level image whereby neighbouring pixels of similar colour/Hue were connected together into one region. These regions were then ranked in order of their total number of pixels. The second largest region was taken to represent the indicator material as the largest represented the background. A binary mask image was created with white pixels set as the indicator region, see Figure 5b. Following this, a binary morphological erosion process [36] was applied to remove edge pixels that may belong to the background and thus interfere with analysis. Figure 5c shows the final step of the segmentation process once the mask was applied to the original image. The average of every identified pixel's hue component is taken to representing the pH at a given station.

3.3 Experimental Procedure

First, a comparison is drawn between using the RGB and HSI colour spaces to investigate which model was more robust to light variation. To do this, the camera was maintained in a fixed position in an area of variable lighting intensities with the colour checker chart in view for reference (Figure 8a), and a number of changes in the lighting applied to investigate the robustness of the colour determination, see Section 4.1 and Figure 8d.

Next it was necessary to investigate the camera response to pH induced colour changes. WANDA was kept stationary in the water container allowing for a continuous view of one pH station, see Figure 9 for setup. Next, ca. 5 ml of the HCl solution was injected using a standard 5 ml pipette around the sensing station causing a colorimetric change of the pH sensor. After that, the indicator was encouraged to return to its original state prior to addition of the acid solution by manually mixing the water in the vicinity of the station to disperse the acid plume. The resulting video

stream was processed and analysed as explained previously in Section 3.2 and a plot of the changing state of the colorimetric sensor from a neutral (green) to an acidic (yellow) state was generated, see Section 4.2 and Figure 10. This process was repeated three times to investigate reproducibility.

To determine if WANDA can detect a chemical event during a patrol, three pH indicator stations, designated as L1, L2 and L3, were placed in different locations within the water container as shown in Figure 11. Software was implemented to achieve an autonomous circular patrol route within the water container with a diameter of ca. 0.7 m. The starting point 'S' was defined to be the starting point and the finishing point WANDA reaches on its circular patrol route when viewed from above. Each station was positioned to be in the camera's field of view as WANDA swims past. Next, a pH plume was injected at station L2 causing a colorimetric change in the pH sensor. Three images of each pH station were processed and analysed as explained in Section 3.2. Finally, the hue value of each sensor station against time was plotted, see Section 4.3, Figures 12 and 13.

4. RESULTS AND DISCUSSION

4.1 Using a Video Camera as a Chemical Detector

Previous studies, as mentioned in Section 2.2, have successfully used a video camera as a pH colorimetric detector. However, these studies have been performed under controlled lighting conditions and using the RGB colour model. A key requirement in this study was that the system should be able to perform under variable ambient lighting conditions. The RGB colour space is inherently sensitive to variations in lighting, and cannot meet this requirement, and thus a more robust method was needed. For this reason the HSI colour space technique was adopted. The transformation from RGB to HSI separates the light intensity 'I' (intensity), colour intensity 'S' (saturation) and colour 'H' (hue) into separate components. By separating the light intensity from the colour, the Hue component is more robust than RGB to variable lighting conditions. To illustrate this, Figures 8a, 8b and 8c show segmentation steps of the colour chart's green patch (chosen as it was the nearest colour to the neutral state of the pH indicator, seen in Figure 5a).

Figure 8d shows the real time plot of the colour reference chart's green path over a period of 450 seconds. During this time deliberate light variation effects were implemented such as shadows at the beginning (0-100 s) and end (350-450 s) and switching on and off the laboratory light at ca. 250 s. This figure (where all component values are normalised between 0 and 1) shows the effects of light intensity variations on the individual Green, Blue, Red and Hue components, ordered from most to least effected. It can be seen that the RGB components do not respond uniformly to the induced lighting effects. The non-uniformity results from a combination of two factors; the light source and the response of the red, green and blue photo sensors within the camera. However the Hue component remains less sensitive to the camera calibration and light source and, as such, is our preferred choice for our analysis during subsequent patrols, see Section 4.3.

4.2 Camera Evaluation

For proving the overall concept hypothesised in this paper we are only interested in two clearly detectable states; neutral 'pH7' and an identifiable acidic 'pH<5' while keeping the detection system robust to variations in lighting. Figure 6 shows the reference chart accompanying the pH indicator. In its neutral state, i.e. pH7, the indicator is green in colour, however when an acid is introduced the colour will shift towards a colour between green and red depending on the concentration of acid and its dispersion in the water.

The camera's response was profiled by analysing the pH strip in its neutral and acidic states. WANDA was kept stationary in the water container with a pH station directly in the camera's field of view (Figure 9). An acidic plume was introduced near the pH station by injecting ca. 5 ml 1 Molar hydrochloric acid, triggering a colour change of the pH indicator material. The indicator pixels in the captured image were extracted using the image processing approach outlined above and the colour change was represented numerically according to the hue angle.

Figure 10 shows the analysis of the dominant Hue colour value of the pH station in the two identifiable states; green in neutral state and yellow when the acidic plume was introduced (a pH change from 7 to ca. 5, see Figures 6 and 7). Figure 10f shows a plot of this change occurring three times. Labels a-e in figure 10f show a correlation to Figure 10 elements (a) – (e), numerically and visually, of the change and recovery at specified times. From figure 10f it can be seen that this process is clearly reproducible and that the colour/Hue is proportional to the level of chemical contaminant. The response is sufficiently clear to enable the two states to be identified. For more accurate analysis we could consider employing noise reduction algorithms such as dropping frames with identifiable noise during image processing.

4.3 Environmental Monitoring – WANDA on Patrol

Once it had been established that the camera can be used to detect the presence of an acid plume in the immediate environment surrounding the pH sensor station, the approach was extended to the use of WANDA in a 'patrol' mode, in which WANDA would follow a set path to check the pH status of the water container by monitoring the colour of several land mark stations.

The three pH stations, labelled (L1, L2, L3), were placed in different areas of the water container and a fixed patrol route defined; starting from point S, passing station 1, 2 and 3 en route and finishing up back at the starting point. Video images were recorded and transmitted wirelessly in real-time to a PC. Image analysis was performed off-line for these experiments, but it is our intention to develop a fully autonomous procedure that will be implemented on the WANDA platform. Three video frames per station were manually selected to investigate reproducibility. These frames are chosen to offer the best quality for analysis i.e. those without any noise obscuring the colorimetric sensor pixel area.

Two separate patrol operations were performed to demonstrate the principle.

Patrol # 1: Normal condition; all landmark stations were green in colour

Patrol # 2: Event occurred; the environment surrounding station L2 was acidified and the station indicated a yellow colour. The remaining two stations remained unchanged to simulate a locally occurring event.

The results from Patrol # 1 were analysed and used as reference for normal condition. Any change in colour on each of the landmark station would therefore be indicative of a change in their respective local chemical environment.

During operation, the individual landmark identity was signified by its specific shape and feature (cylindrical with colour strip) from its surroundings and the time taken to reach it. A specifically shaped colour code could be used for each location if preferred; here we adopted the simplest format to reduce the amount of image analysis for site recognition in this first trial.

Figure 12(a-c) displays an extracted image sequence from the video stream showing that the three indicator stations are green for visual reference. The result of the image analysis (Figure 12d) indicates that the three stations gave a similar green hue output with values of ca. 1.6 rad, in agreement with the initial camera response experiments (see Figure 10f). This data has shown that WANDA – in conjunction with the image analysis technique - was successful in determining the correct status of the colorimetric sensors i.e. that the environmental status of all sensor stations was 'normal'. This information was stored and used as reference for future monitoring operations.

By comparing colour/hue state of indicator stations in future patrols with the reference data one can therefore provide information about changes in the local pH. This is demonstrated here in the case of Patrol # 2. The exact same method for Patrol # 1 was employed to produce video images and colour information for Patrol # 2, shown in Figures 12 and 13 respectively. The captured images (Figures 12a, 12c, 13a and 13c) show that stations L1 and L3 remain unchanged, whereas station L2 (Figures 12b and 13b) has changed from green to yellow, visually indicating that the sensor has responded to a change in pH in the environment immediately surrounding station L2 and that this contaminant was localised because it did not affect stations L1 or L3. The results of the image analysis (Figures 12d and 13d) indicates that the two stations L1 and L3 gave similar green hue output (ca. 1.6 rad) as previously recorded, whereas L2 has changed its reported hue output from ca. 1.6 rad to ca. 0.7 rad. Hence the change in sensor colour was successfully captured by WANDA.

A more robust and simple technique has also been developed to determine if an event has occurred. It is based on comparing the hue value of each respective sensor stations between different patrols through comparison of the ratio of the sensor hue values between runs. For comparison, a single hue value is taken to represent each sensing station; i.e. the hue average of the 3 captured images of a single sensing station is calculated and is representative the station's pH state. Next, the hue ratio of each respective sensing station is calculated e.g. ratio of L1 (Patrol # 1) to that of L1 (Patrol # 2). Figure 14 shows the plot of the hue ratio of respective sensors between Patrol # 1 and Patrol # 2. The results clearly show that when there was no change in the pH environment, the colour ratio of the sensor stations (L1 and L3) were very close to 1. Meanwhile a ratio value of > 2 was obtained for L2 where a pH change in environment was induced. This demonstrates that WANDA has successfully reported a chemical change in the local environment.

This simple analysis technique can be made useful for detecting minor changes in a pH environment by setting a threshold value of how far the ratio deviates from normal conditions (e.g. 5% deviation from ratio = 1), resulting in a semi quantitative mobile warning system for detecting localized events in target areas.

4.4 Significance and Future Developments

The significance of the approach demonstrated in this paper to the realisation of water quality monitoring sensing networks is that it potentially allows for a significant cost reduction of infrastructure and maintenance. The need for power, communications, and processing units is no longer necessary for individual sensor stations. As a result, this model is inherently more scalable than traditional techniques and as such allows for wider areas to be sensed meeting the needs of future legislation. Other areas where this type of technology may be useful include; port monitoring for oil spillages, air quality in hazardous workplaces, food preparation surroundings, detection of threats (e.g. detection of release of chem./bio-warfare agents) using mobile or fixed cameras. For example, low cost colorimetric sensors could be deployed within water catchments areas or aquariums where ammonia levels increases with biological waste. If the continuously operating filtration system breaks down without a monitoring technique in place, such as the approach offered in this paper, it can result in heavy cost and loss of fish life.

As this concept is in its early stage, numerous improvements can be introduced. Since the patrol route was fixed; the order/time at which the stations were encountered was used for identification purposes. Although it is not needed in this paper, a real deployment will rely on shape and/or a colour coded pattern design as a discriminating factor. The chemical indicator stations can be designed with a unique 3D shape/colour id with a high contrast to anything in its environment for location/identification purposes.

Noise is an unavoidable problem for any system. For the approach in this paper, i.e. using a wireless camera for chemical analysis, image quality is paramount. Limitations of using wireless cameras have been outlined by Byrne et all [37], where one faces challenges such as range, chromatic noise, horizontal scan line noise and visible vertical blanking due to vertical sync loss. Such challenges have been encountered in this study i.e. visible in plots Figures 8d and 10f shown as grey lines. Methods to overcome these problems can include noise identification in video frames (mentioned in Section 4.2) and/or to perform image and video processing on the device itself (mentioned in Section 4.3) whereby an autonomous regime can be implemented on WANDA allowing for flexibility towards true autonomy without range limitations.

Improvements to the platform itself are also foreseen. At present, WANDA is limited to low flow rate areas in its current implementation. Enhancements may include; the development of a more streamline casing to accommodate higher flow rates, investigation into new PPy arrangements for greater efficiency or even replacement of the propulsion method with a more conventional system. However replacing the propulsion may impact on deployment life-time due to a higher power draw e.g. a motor with directional control.

Multiple dye-based sensors immobilised on a single station will enable the status of multiple components and numerous locations to be monitored. Establishing colour references on stations in conjunction with adaptive training techniques will help with any potential biological fouling or medium discolouration encountered in long term real deployments. Further research into how this detector will behave with drastically changing lighting conditions in a real environment, e.g. night time, is clearly

necessary. In addition, generating more robust quantitative data will be necessary before real deployments can be expected to be productive.

5. CONCLUSIONS

This work reports the successful demonstration of a novel approach to chemical sensing networks. A low cost, biomimetic robotic fish was used to patrol a water container in a laboratory and inspect static chemical sensor stations en route. A first patrol was used as a reference for normal conditions. During a second patrol, a contaminant was added in the vicinity of one of the stations. By applying a sequence of image processing techniques to the captured video stream, the presence of the pH plume was successfully identified. While this study comprised of three stations with one colorimetric sensor on each, the approach is potentially scalable to numerous stations fitted with multiple sensors for a range of possible contaminants. Moreover with evolving CCD technology, power efficiency and processing power; it is feasible that the entire detection-processing algorithm will be integrated onto the autonomous vehicle in the near future.

ACKNOWLEDGEMENTS

This work was supported by Science Foundation Ireland under the Clarity: Centre for Sensor Web Te1chnologies (grant 07/CE/I1147) and the Australian Research Council.

REFERENCES

[1] Hoyer, M.V., et al., (2009), "Fish Kills in Florida's Canals, Creeks/Rivers, and Ponds/Lakes", *J.Aquat.Plant Manage.,* Vol.47 pp. 53-56.

[2] Al-Bahry, S.N., et al., (2009), "Coastal sewage discharge and its impact on fish with reference to antibiotic resistant enteric bacteria and enteric pathogens as bio-indicators of pollution", *Chemosphere,* Vol.77 (11), pp. 1534-1539.

[3] Brian Austin., (2007), "The involvement of pollution with fish health", *in Anonymous* pp. 13-30.

[4] Zulima Palacio. Fish Kills Linked to Water Pollutants. 2009 2009-19-10;2010(March/08):1.

[5] James Hayden. Fisheries officials investigate Tipperary fish kill. The Irish Times 2009 Thursday, July 2, 2009.

[6] Wainwright, M. Pollution kills fish in waterways. The Guardian UK 2003 Wednesday 4 June 2003;Environment.

[7] EU Water Framework Directive, [online], http://www.wfdireland.ie/.

[8] Office of Ground Water and Drinking Water (OGWDW), [online], http://www.epa.gov/OGWDW/.

[9] Water Quality Association, [online], http://www.wqa.org/.

[10] EPA. Water Quality In Ireland 2007-2008 : Key Indicators of the Aquatic Environment. 2009;978-1-84095-319-0:1-52.

[11] Diamond, D. (2004), "Internet-scale sensing", *Anal.Chem.,* Vol.76 (15), pp. 278A-286A.

[12] Diamond, D., et al., (2008), "Integration of analytical measurements and wireless communications - Current issues and future strategies", *Talanta,* Vol.75 (3), pp. 606-612.

[13] McGraw, C.M., et al., (2007), "Autonomous microfluidic system for phosphate detection", *Talanta,* Vol.71 (3), pp. 1180-1185.

[14] Hayes, J., et al., 2007, "Intelligent Environmental Sensing with a Phosphate Monitoring System and Online Resources", "Intelligent Environmental Sensing with a Phosphate Monitoring System and Online Resources", *COMPUTATION IN MODERN SCIENCE AND ENGINEERING: Proceedings of the International Conference on Computational Methods in Science and Engineering 2007 (ICCMSE 2007),*Vol.963, *12/2007,*: American Institute of Physics 1216-1219.

[15] Cleary, J., et al., (2008), "An autonomous microfluidic sensor for phosphate: On-site analysis of treated wastewater", *IEEE Sens.J.,* Vol.8 (5-6), pp. 508-515.

[16] McGovern, S., et al., (2009), "Finding NEMO (novel electromaterial muscle oscillator): a polypyrrole powered robotic fish with real-time wireless speed and directional control", *Smart Mater.Struct.,* Vol.18 (9), pp. 095009.

[17] Zhang, D.S.and Lu, G.J., (2004), "Review of shape representation and description techniques", *Pattern Recognit,* Vol.37 (1), pp. 1-19.

[18] Smela, E., Inganas, O.and Lundstrom, I., (1993), "Conducting polymers as artificial muscles: challenges and possibilities", *J Micromech Microengineering,* Vol.3 (4), pp. 203.

[19] Durrant-Whyte, H.and Bailey, T., (2006), "Simultaneous localization and mapping: Part I", *IEEE Robot.Autom.Mag.,* Vol.13 (2), pp. 99-108.

[20] Bailey, T.and Durrant-Whyte, H., (2006), "Simultaneous localization and mapping (SLAM): Part II", *IEEE Robot.Autom.Mag.,* Vol.13 (3), pp. 108-117.

[21] BYRNE, L., et al., 2001, "Digital imaging as a detector for quantitative colorimetric analyses", *Society of Photo-Optical Instrumentation Engineers, Bellingham, WA, ETATS-UNIS, ed., Proceedings of SPIE, the International Society for Optical Engineering,*Vol.4205, *2001,*: SPIE INIST-CNRS, Cote INIST : 21760, 35400013481602.0330, 267-277.

[22] Lau, K.T., Edwards, S.and Diamond, D., (2004), "Solid-state ammonia sensor based on Berthelot's reaction", *Sens.Actuator B-Chem.,* Vol.98 (1), pp. 12-17.

[23] Safavi, A., et al., (2007), "CCD camera full range pH sensor array", *Talanta,* Vol.71 (1), pp. 498-501.

[24] Stich, M.I.J., et al., (2009), "Read-out of multiple optical chemical sensors by means of digital color cameras", *Sens.Actuator B-Chem.,* Vol.139 (1), pp. 204-207.

[25] Hayes, J., et al., 2006, "Web-based colorimetric sensing for food quality monitoring", "Web-based colorimetric sensing for food quality monitoring", *Sensors, 2006. 5th IEEE Conference on, 22-25 Oct. 2006,*: IEEE Daegu, 855-858.

[26] Wireless camera ZT-830T product page, [online], http://www.rapserv.com.au/prod4944.htm (Accessed 31/03/2010).

[27] EZ Radio ER900TRS Datasheet (available as a downloadable document), [online], http://www.datasheetarchive.com/datasheet-pdf/078/DSAE0066545.html (Accessed 31/03/2010).

[28] Sun Microsystems. Java Runtime Edition.

[29] Sun Microsystems. Java Communications Package.

[30] Humatic Media Tools. DirectShow Java Wrapper.

[31] Sun Microsystems. Java Advanced Imaging (JAI). ;2010(10/03/2010):1.

[32] J.J. BARDYN et al. 1984, "Une architecture VLSI pour un operateur de filtrage median", "Une architecture VLSI pour un operateur de filtrage median", *CONGRES RECONNAISSANCE DES FORMES ET INTELLIGENCE ARTIFICIELLE,*Vol.1, *25th - 27th January 1984,* Paris, 557-566.

[33] SUN Microsystems., (1999)*, Programming in Java Advanced Imaging,* (1st ed.), SUN Microsystems,.

[34] Smith, A. R. 1978, "Color gamut transform pairs", "Color gamut transform pairs", *SIGGRAPH '78: Proceedings of the 5th annual conference on Computer graphics and interactive techniques,*: ACM New York, NY, USA, 12-19.

[35] Fortner, B. and Meyer, T.E., (1997)*, Number by colors : a guide to using color to understand technical data,* (1st ed.), TELOS, Electronic Library of Science, Santa Clara, Calif.

[36] Gonzalez, R.C. and Woods, R.E., (2002)*, Digital image processing,* (2nd ed, international ed. ed.), Prentice Hall, Upper Saddle River, NJ.

[37] Byrne, J. and R. Mehra 2008, "Wireless Video Noise Classification for Micro Air Vehicles", "Wireless Video Noise Classification for Micro Air Vehicles", *Proceedings of the 2008 Association for Unmanned Vehicle Systems International (AUVSI) Conference, June 10-12, 2008,*: AUVSI.

LIST OF FIGURES

green patch region after applying the binary mask image to the original captured image. (d) Real time plot of the colour reference chart's green patch over a period of 450 s, showing the response of the Red, Green, Blue and Hue components. Smoothing (heavy lines) applied to raw captured data (grey lines) for visualisation purposes.

Figure 9. Layout of pH station and WANDA within the water container for profiling the response of the camera to induced pH changes of the water surrounding a sensing station. See Figure 5a for a similar captured view of the sensing station.

Figure 10. Image sequence and response plot showing reaction to addition of acid near a sensor station. (a) Before acidification. (b) During acidification. (c) Acidified. (d) Recovering. (e) Recovered. (f) Real time response plot of the camera's hue analysis of the sensing station to 3 induced pH changes over time. Labels 'a' – 'e' correspond to figure elements 'a – e' respectively. Smoothing (black line) applied to raw captured data (grey line) for visualisation purposes.

Figure 11. Layout of pH stations and patrol route within the water container. 'S' starting and ending point of the patrol route, 'L1' pH station 1, 'L2' pH station 2, 'L3' pH station 3. (a) Plan view diagram of patrol route of sensing platform. (b) Corresponding photographic image for reference.

Figure 12. Image sequence and response plot showing the response of camera to all three pH sensing stations during Patrol # 1 'normal conditions' in the water container. (a) Three captured video frames of pH station L1 as WANDA swims past. (b) Three captured video frames of pH station L2 as WANDA swims past. (c) Three captured video frames of pH station L3 as WANDA swims past. (d) Response plot of the camera's hue analysis of sensing stations L1, L2 and L3 corresponding to figure elements (a) – (c).

Figure 13. Image sequence and response plot showing the response of camera to all three pH sensing stations during Patrol # 2 'change in local pH conditions' in the water container. (a) Three captured video frames of pH station L1 as WANDA swims past. (b) Three captured video frames of pH station L2 as WANDA swims past. (c) Three captured video frames of pH station L3 as WANDA swims past. (d) Response plot of the camera's hue analysis of sensing stations L1, L2 and L3 corresponding to figure elements (a) – (c).

Figure 14. Comparison of Patrol # 1 and Patrol # 2. A single hue value is taken to represent each sensing station. Points represent the average hue ratio of station's L1, L2 and L3. Upper and lower error bars represent the max and min hue ratio respectively.

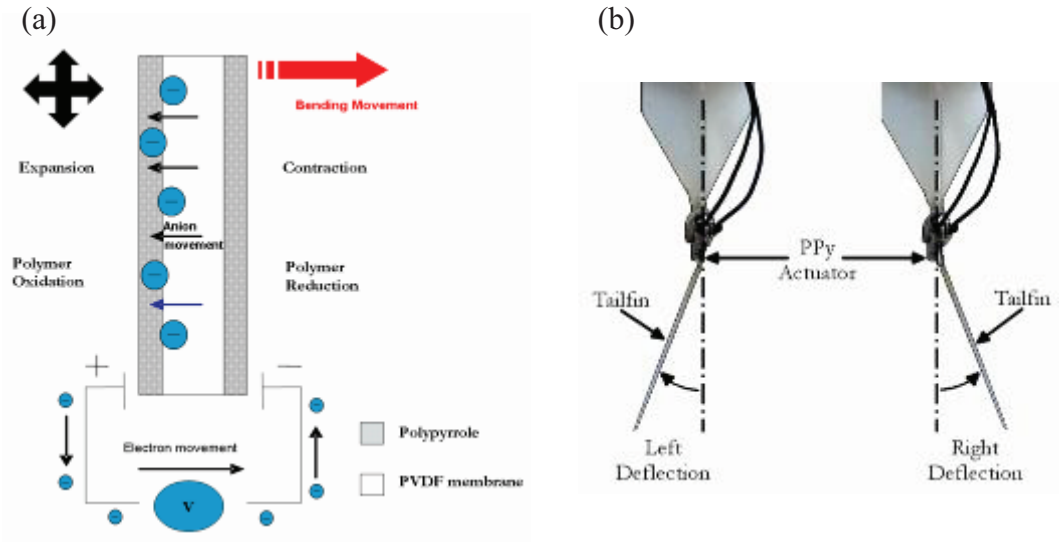

Figure 1. (a) Cross sectional diagram showing bending principle of the tri-layer conducting polymer actuators. Applying a low electrical potential 'V' causes oxidation of one polypyrrole layer and reduction of the other resulting in a bending movement. (b) Images showing the resulting bending movement of WANDA's polymer actuators when a rigid tailfin is attached.

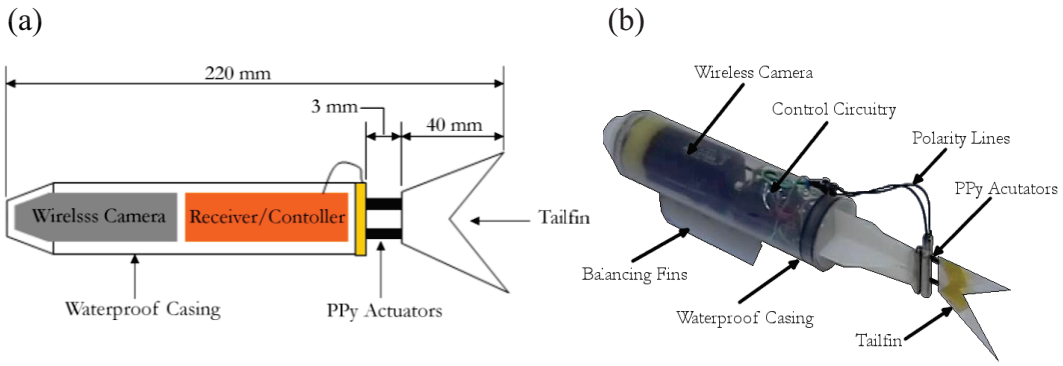

Figure 2. (a) Diagram showing the wireless camera, controller, casing, PPy actuators, and tailfin arrangement on the WANDA device. Dimensions added for size reference. (b) Image of WANDA assembly for visual reference. Major components labelled including left balancing fin (right balancing fin obscured from view).

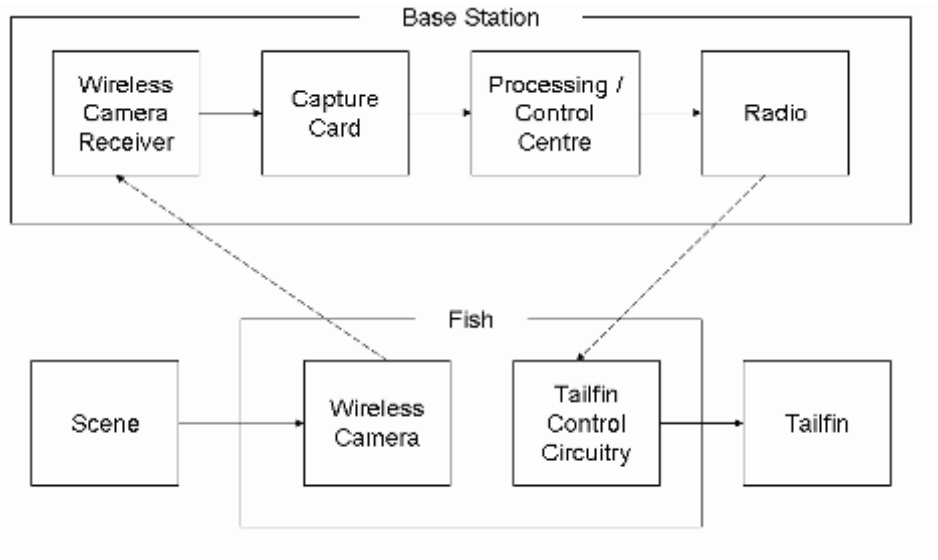

Figure 3. Block diagram illustrating the full closed loop control system of WANDA and sub unit interactions thereof. A captured 'Scene' is relayed via the 'Wireless Camera' on the 'Fish' to the 'Wireless Camera Receiver' on the 'Base Station'. The 'Capture Card' forwards the image to a PC or 'Processing/Control Centre' where it extracts and analyses data. Decisions are made based on this data and forwarded via the 'Radio' to the 'Tailfin Control Circuitry' on board the 'Fish' where it alters the 'Tailfin' state resulting in controlled directional movement.

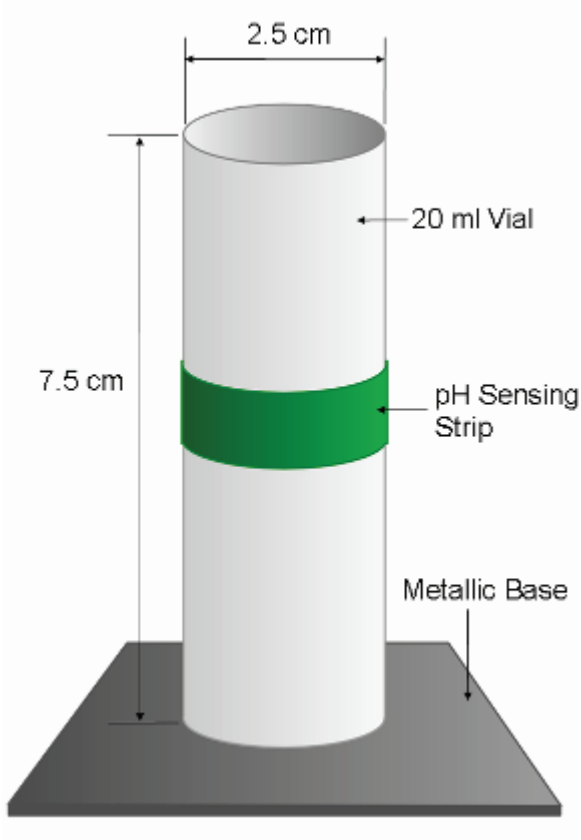

Figure 4. Diagram showing the construction of a pH sensing station used during patrols. A standard 20 ml cylindrical vial is affixed to a heavy metallic base used as an anchor. One strip of universal pH indicator coated with ethyl cellulose is attached around the centre of the vial. Dimensions added for size reference.

Figure 5. Segmentation process to selectively extract the pH indicator region of the test station in the water container. (a) Single captured image of a pH sensing station from the wireless camera. (b) Generated binary mask image after applying region segmentation image processing algorithms. White pixels representing the pH sensing strip region. (c) Resulting image of the extracted pH indicator region after applying the binary mask image to the original captured image.

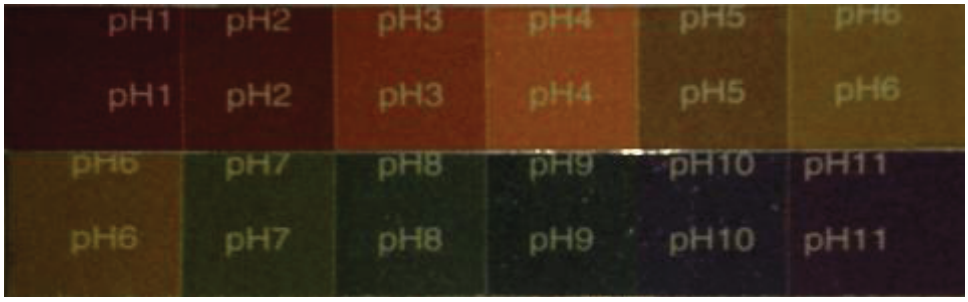

Figure 6. Image showing the reference chart accompanying the pH indicator (Johnson Universal pH Indicator).

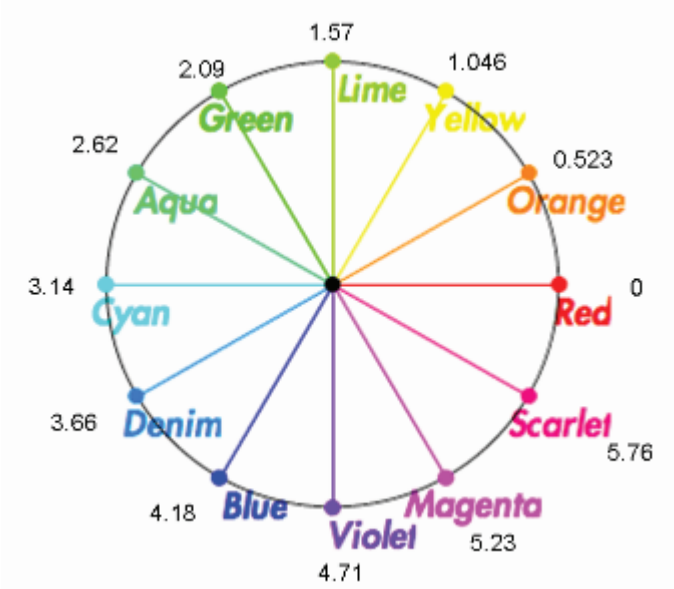

Figure 7. Hue channel of the HSI colour space [34] normalised between 0 and 2π. Image shows quantitative values in relation to common colours at 30˚ (0.523 rad) intervals.

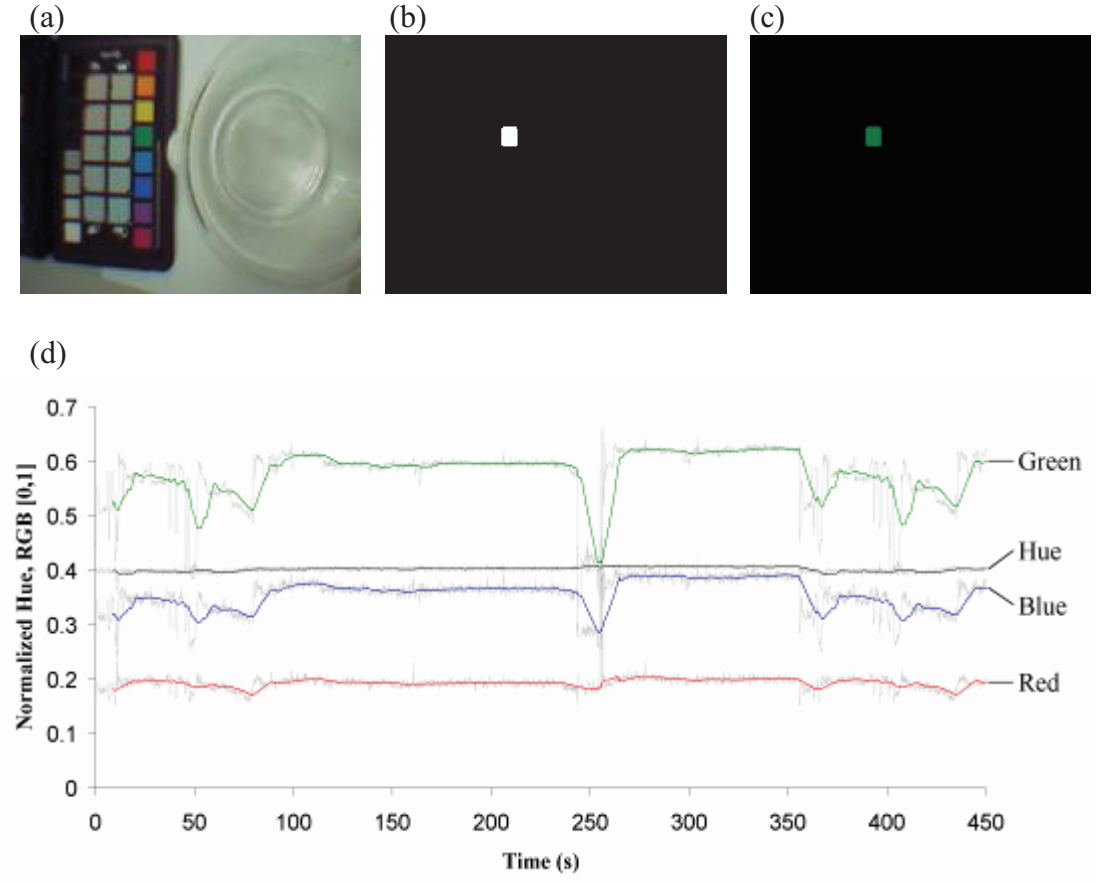

Figure 8. Segmentation and evaluation process to selectively extract a reference colour patch, analyse it under induced light intensity variations and compare the RGB and HSI colour spaces. (a) Single captured image of the X-Rite colour reference chart from the wireless camera. (b) Generated binary mask image after applying region segmentation image processing algorithms. (c) Resulting image of the extracted green patch region after applying the binary mask image to the original captured image. (d) Real time plot of the colour reference chart's green patch over a period of 450 s, showing the response of the Red, Green, Blue and Hue components. Smoothing (heavy lines) applied to raw captured data (grey lines) for visualisation purposes.

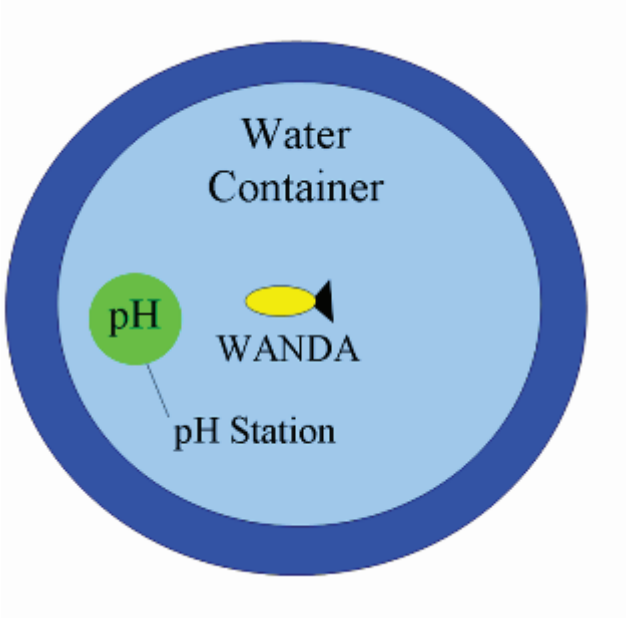

Figure 9. Layout of pH station and WANDA within the water container for profiling the response of the camera to induced pH changes of the water surrounding a sensing station. See Figure 5a for a similar captured view of the sensing station.

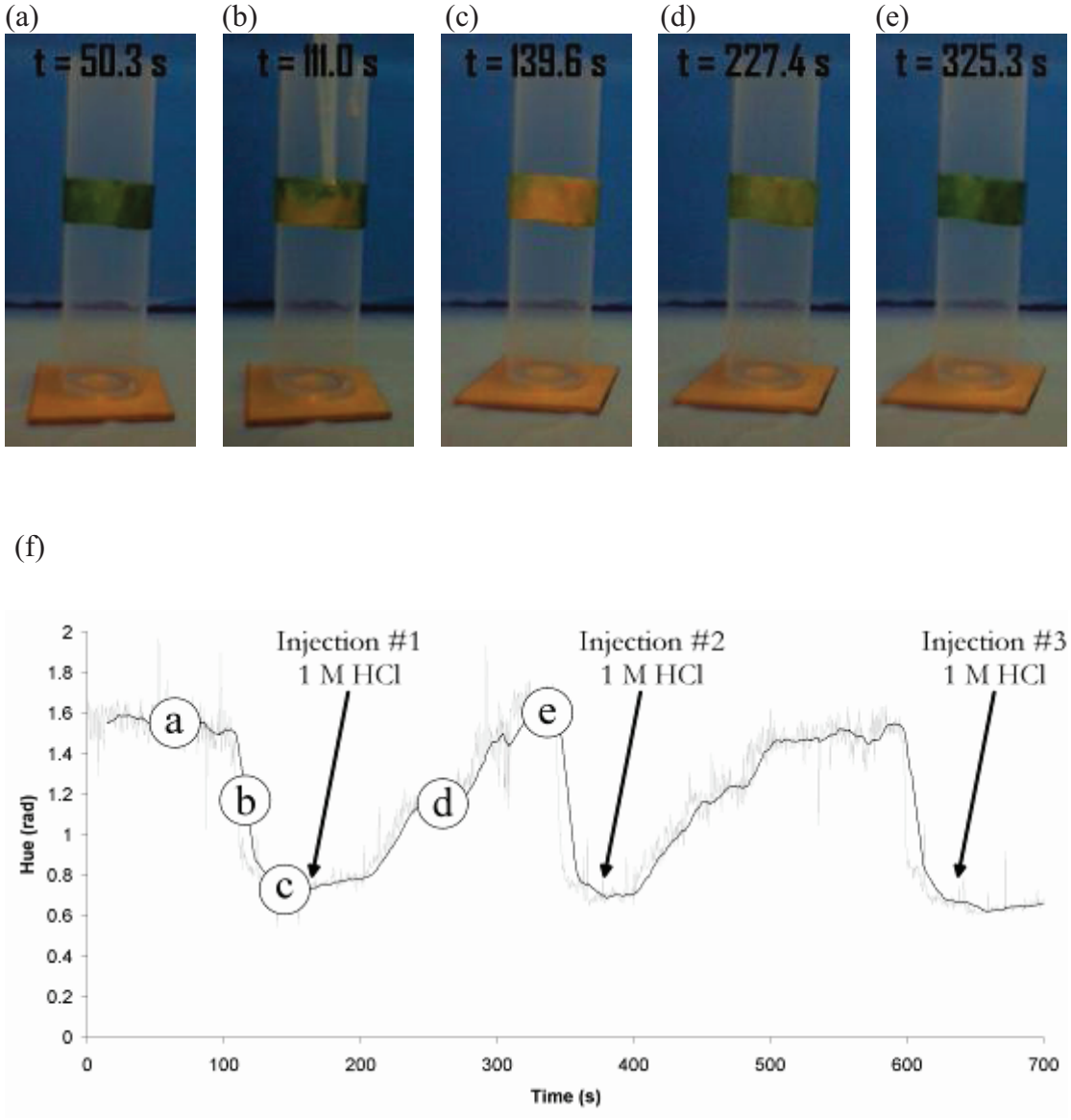

Figure 10. Image sequence and response plot showing reaction to addition of acid near a sensor station. (a) Before acidification. (b) During acidification. (c) Acidified. (d) Recovering. (e) Recovered. (f) Real time response plot of the camera's hue analysis of the sensing station to 3 induced pH changes over time. Labels 'a' – 'e' correspond to figure elements 'a – e' respectively. Smoothing (black line) applied to raw captured data (grey line) for visualisation purposes.

(a) (b)

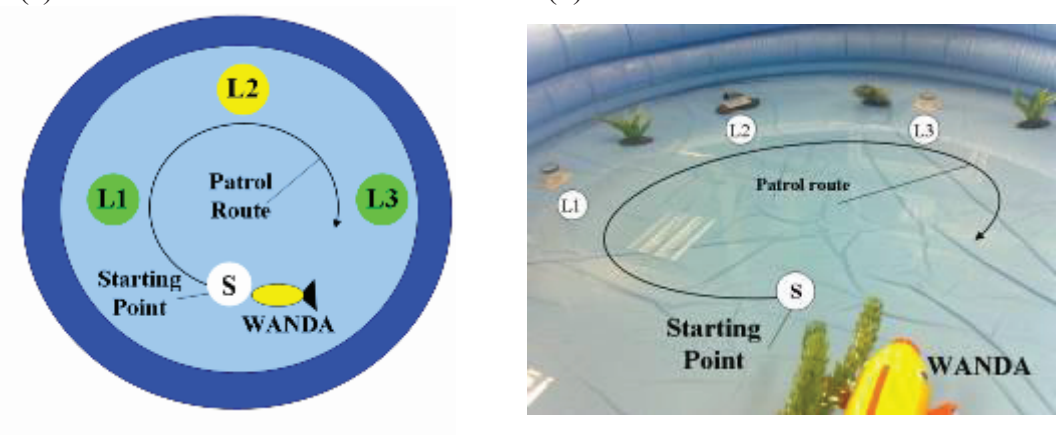

Figure 11. Layout of pH stations and patrol route within the water container. 'S' starting and ending point of the patrol route, 'L1' pH station 1, 'L2' pH station 2, 'L3' pH station 3. (a) Plan view diagram of patrol route of sensing platform. (b) Corresponding photographic image for reference.

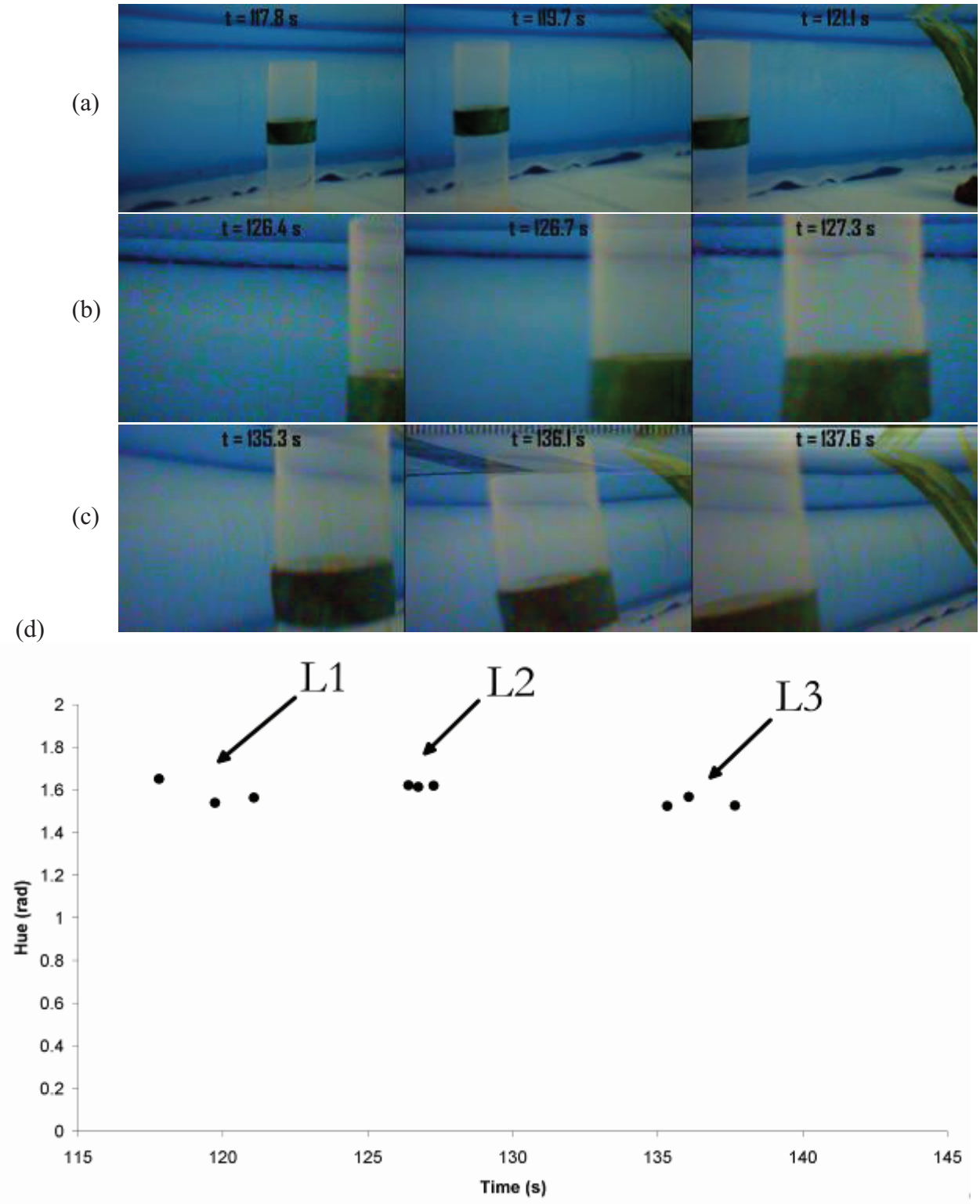

Figure 12. Image sequence and response plot showing the response of camera to all three pH sensing stations during Patrol # 1 'normal conditions' in the water container. (a) Three captured video frames of pH station L1 as WANDA swims past. (b) Three captured video frames of pH station L2 as WANDA swims past. (c) Three captured video frames of pH station L3 as WANDA swims past. (d) Response plot of the camera's hue analysis of sensing stations L1, L2 and L3 corresponding to figure elements (a) – (c).

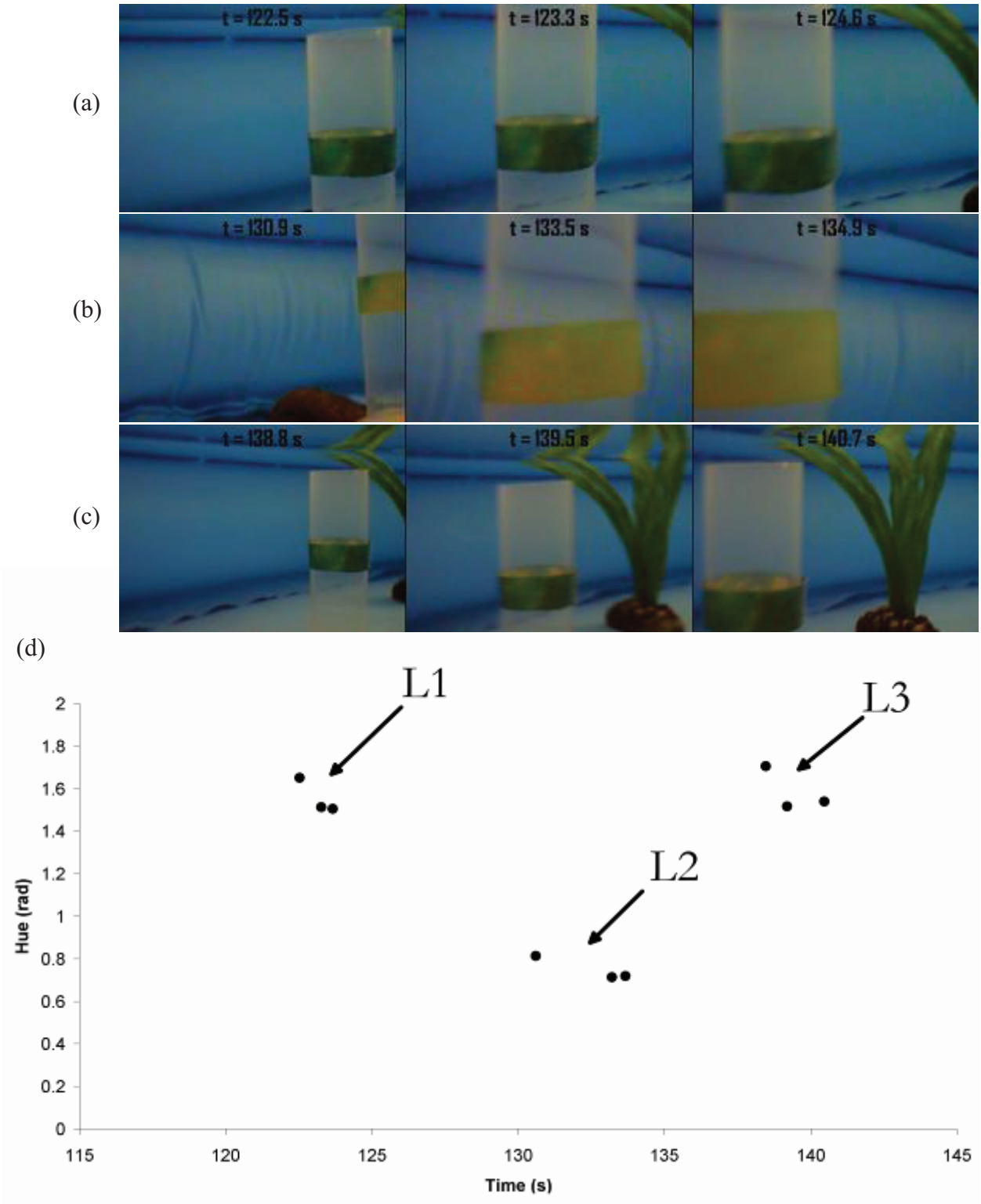

Figure 13. Image sequence and response plot showing the response of camera to all three pH sensing stations during Patrol # 2 'change in local pH conditions' in the water container. (a) Three captured video frames of pH station L1 as WANDA swims past. (b) Three captured video frames of pH station L2 as WANDA swims past. (c) Three captured video frames of pH station L3 as WANDA swims past. (d) Response plot of the camera's hue analysis of sensing stations L1, L2 and L3 corresponding to figure elements (a) – (c).

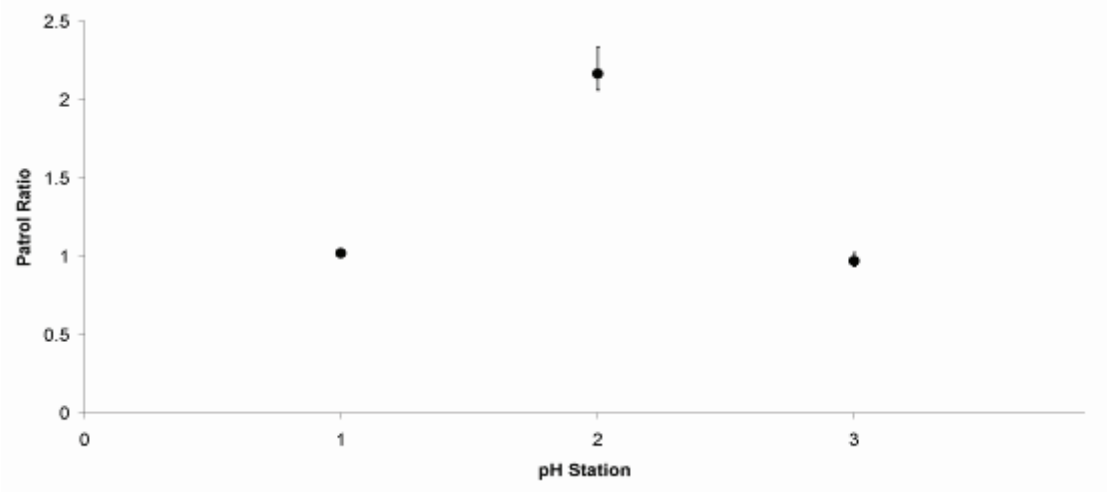

Figure 14. Comparison of Patrol # 1 and Patrol # 2. A single hue value is taken to represent each sensing station. Points represent the average hue ratio of station's L1, L2 and L3. Upper and lower error bars represent the max and min hue ratio respectively.